ChemElectroChem

Research Article
doi.org/10.1002/celc.202400411

Chemistry Europe
European Chemical Societies Publishing

www.chemelectrochem.org

Ionic Diode Current Rectification in High Salt Media with Sulfonated Poly(oxy-1,4-phenylene-oxy-1,4-phenylenecarbonyl-1,4-phenylene)

Chhavi Sharma,[a, b] Sara E. C. Dale,[a] Klaus Mathwig,[c] Marcel A. G. Zevenbergen,[c] Zhongkai Li,[d] Bhuvanesh E.,[e] Kaushik Parida,[b] Yuvraj Singh Negi,[b] and Frank Marken*[d]

Sulfonated poly(oxy-1,4-phenylene-oxy-1,4-phenylenecarbonyl-1,4-phenylene) also known as SPEEK is a chemically robust cation conductor with good solution processability. A thin film (approx. 0.7 μm) coated asymmetrically over a 10 μm diameter microhole in a Teflon substrate film (5 μm thickness) produces ionic diode effects in aqueous electrolyte media even at high ionic strengths up to 2 M NaCl. The enhancement in the ionic diode performance under high salt conditions is tentatively attributed to a (partial) switch from a concentration polarisation effect (dominant for high diode currents) to interfacial polarisation (dominant at low current; proposed for molecularly rigid ionomers). Ionic strength effects on the diode performance seem relatively low further indicative of a mechanism for the diode effect caused by interfacial polarisation without significant concentration polarisation. Preliminary comparison of diode phenomena in aqueous HCl, LiCl, NaCl, and $MgCl_2$ reveals cation specific effects due to interaction with the polymer.

1. Introduction

Ionic diode processes in electrochemical microfluidic systems[1,2] are observed when (condition I) asymmetry is imposed and when (condition II) a potential dependent structural change occurs.[3] There are many types of asymmetry contributing to the ionic diode effect (solution phase asymmetry,[4] nanocones,[5,6] pipettes,[7] asymmetric coatings,[8,9] *etc.*) and many types of potential-triggered structural changes (depletion and accumulation of charge carriers,[10] depletion and accumulation of electrolyte in concentration polarisation,[11] proton-hydroxide annihilation,[12] precipitation reactions,[13] and other types of potential triggered structural changes). Applications for ionic diodes have been proposed in desalination,[14] in dialysis,[15] water pumping,[16] chemical analysis and sensing,[17,18] and in ionic circuits.[19,20]

Microfluidic ionic diodes provide ionic current rectification effects, but suffer from low efficiency at high salt concentration (which can be problematic for example in desalination,[21,22] in salinity gradient power generation,[23] or in ionic logic devices[24]). In the development of microscale ionic diodes (often microhole devices[25]) based on for example Nafion,[26] graphene oxide,[27] Aquivion,[28] Sustainion,[29] or on bacteriophage derived ionomer,[30] the concentration polarisation effect has been exploited, but this is inefficient at high salt concentrations. Only more recently has work been reported on a polymer of intrinsic microporosity with quaternised amines cation sites[31] with ultrahigh rectification ratio, with relatively low diode currents, and with a low impact of ionic strength on diode currents. The associated change in diode mechanism from "concentration polarisation" to "interfacial polarisation" was tentatively assigned to molecular rigidity in the ionomer backbone. This observation is followed up here in this study by exploration of the ionic diode characteristics of a SPEEK ionomer.

Sulfonated poly(oxy-1,4-phenylene-oxy-1,4-phenylenecarbonyl-1,4-phenylene) or SPEEK (see molecular structure in Figure 1A) has been employed previously for example in fuel cells,[32] in redox flow cells,[33] or in flue gas dehydration.[34] SPEEK offers an attractive engineering material with chemically robust nature[35] and tunability of the charge carrier concentration (or the equivalent weight).[36] In the context of ionic diodes, SPEEK could provide a chemically robust and molecularly different/more uniform material when compared for example to Nafion,[37] which is known to undergo self-assembled into hydrophilic channels.

[a] C. Sharma, S. E. C. Dale
Department of Physics, University of Bath, Claverton Down, Bath BA2 7AY, UK

[b] C. Sharma, K. Parida, Y. S. Negi
Department of Polymer and Process Engineering, Indian Institute of Technology Roorkee, Saharanpur Campus, Saharanpur 247001, Uttar Pradesh India

[c] K. Mathwig, M. A. G. Zevenbergen
imec within OnePlanet Research Center, Bronland 10, Wageningen 6708 WH, The Netherlands

[d] Z. Li, F. Marken
Department of Chemistry, University of Bath, Claverton Down, Bath BA2 7AY, UK
E-mail: f.marken@bath.ac.uk

[e] B. E.
Department of Research and Technical Support, Permionics Global Technologies LLP., Vadodara, Gujarat 390016, India

Supporting information for this article is available on the WWW under https://doi.org/10.1002/celc.202400411

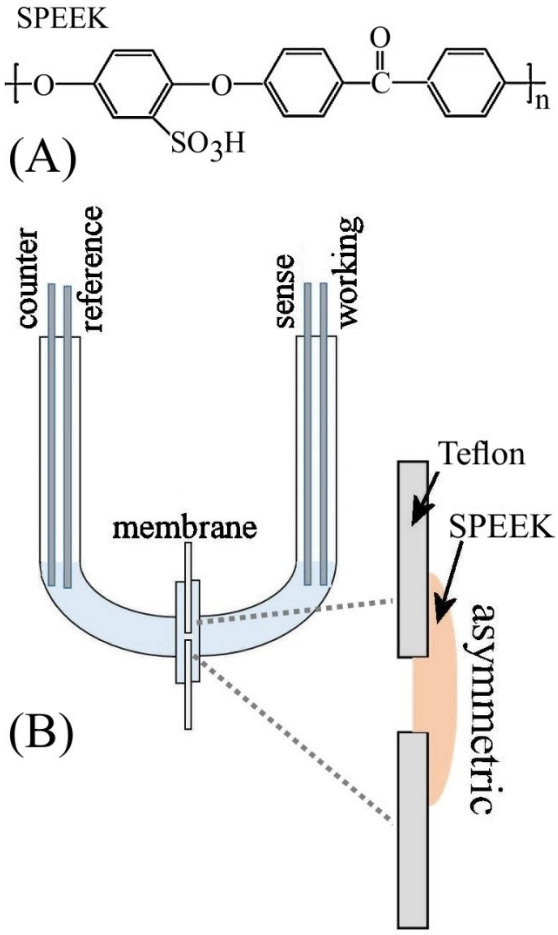

Figure 1. (A) Molecular structure of sulfonated poly(oxy-1,4-phenylene-oxy-1,4-phenylenecarbonyl-1,4-phenylene) (SPEEK). (B) U-cell configuration for ionic diode experiments in 4-electrode mode.

Here, SPEEK is employed as an ionomer in a microhole ionic diode. A methodology is developed to apply a thin film of SPEEK to a Teflon substrate with 10 μm diameter microhole. The sulfonation makes SPEEK a cation conductor similar to Nafion, but with a different molecular structure. The molecular backbone for SPEEK is relatively rigid, and this affects properties such as polymer chain movement contributing to charge transport and/or formation of electric field gradients. Figure 2 illustrates the conditions in a microhole ionic diode (hypothetical) focusing on two extreme limiting cases: (A,B) concentration polarisation in the solution phase and (C) interfacial polarisation (concentrated in the microhole region) causing charge carrier depletion within the ionomer.

The concentration polarisation effect (see microhole region in Figure 2A and B) occurs for all (highly ion-conductive) semipermeable membranes with sufficient ion flow.[38] For ion transport from the membrane into the solution phase, accumulation of salt occurs in the vicinity of the interface (associated with a decrease in resistance). In contrast, for reverse ion flow from solution into the membrane, electrolyte depletion occurs (associated with an increase in resistance). Effects are pronounced in the microhole as indicated here. Electroneutrality is generally maintained in bulk phase. Computational finite element models have been employed to illustrate this case.[39] However, for some rigid ionomer materials (Figure 2C) interfacial polarisation may occur due to localised extraction of mobile charge carriers from the rigid membrane material. Electroneutrality is not maintained. Concentration polarisation is associated with high currents (dominated by diffusion-migration within the microhole), whereas interfacial polarisation is associated with lower currents and loss of the applied voltage at the interface. Importantly, interfacial polarisation should be affected by the molecular structure of the ionomer and thereby allow ion selectivity in diodes.

In this study, it is shown that microhole ionic diodes can become more efficient (with high rectification ratio even for highly saline media) as long as interfacial polarisation (IP) occurs. A partial transition from concentration polarisation (CP) to interfacial polarisation (IP) is suggested due to molecular rigidity of the ionomer material SPEEK. The molecular rigidity of the ionomer is crucial in improving diode performance at high ionic strengths.

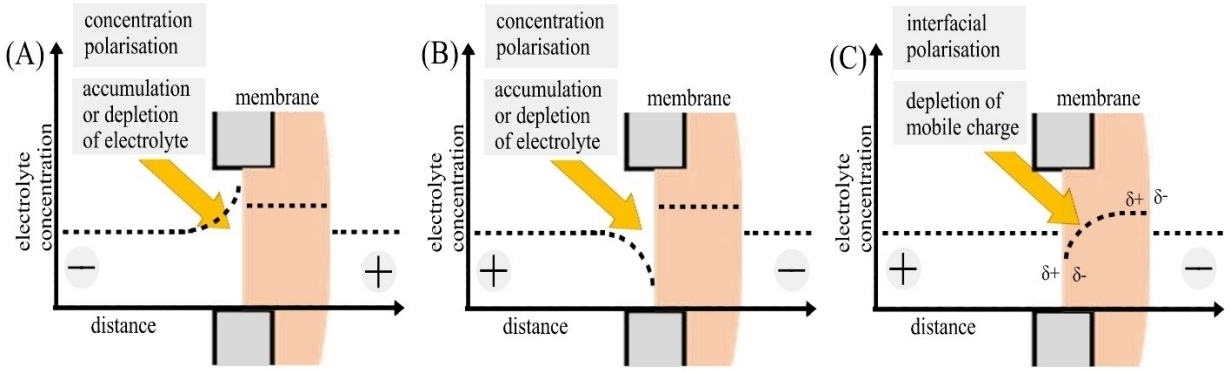

Figure 2. Schematic of (A,B) concentration polarisation in the electrolyte within the microhole region causing ionic diode phenomena for a cationic diode (cations are the mobile species). (C) Interfacial polarisation (hypothetical) within the polymer membrane causing ionic diode phenomena. The applied voltage is indicated by "+" and "−" symbols.

Experimental

Reagents

Poly-(oxy-1,4-phenylene-oxy-1,4-phenylenecarbonyl-1,4-phenylene) (PEEK, KetaSpire KT-820 SFP, Solvay), N-methyl-2-pyrrolidone (NMP, ACS reagent, ≥99.5%, Sigma Aldrich), agarose (Melford Ltd.), sodium chloride (NaCl, 99.5%, Fisher Scientific Ltd.), lithium chloride (LiCl, 99.5%, Sigma Aldrich), magnesium chloride ($MgCl_2$, Sigma Aldrich), HCl (37%, Sigma Aldrich) were obtained commercially and used without further purification. Aqueous solutions were prepared with ultra-pure water from a CE Instruments water purification system, with a resistivity not less than 18.2 MΩ cm at 20 °C.

Instrumentation

Electrochemical characterisation including cyclic voltammetry and chrono-amperometry were performed on a Solartron Analytical ModuLab^{XM} MTS system, with a four-electrode configuration electrochemical cell. The membrane electrochemical cell (Figure 1B) consisted of two cylindrical half-cells, separated by a 5 μm thick Teflon substrate (purchased from Laser Machining Ltd, Birmingham, UK), which was laser-drilled with a microhole (diameter approx. 10 μm). Carbon rods (1 mm diameter) served as both working and counter electrodes and silver wires (0.5 mm diameter) were applied as both quasi-reference and quasi-sense electrodes. During all measurements, the working and sense electrodes were placed into the compartment on the membrane coating side of the cell (Figure 1B) to define the polarity of the applied voltage. Field emission scanning electron microscopy (FE-SEM) was carried out on a MIRA3 TESCAN FESEM with secondary electron detector and with 10 kV acceleration voltage.

Infrared spectra were obtained with a FTIR PerkinElmer system (USA) in attenuated total reflectance (ATR) mode in the range of 4000 cm^{-1}–400 cm^{-1}. X-ray diffraction data (XRD) were obtained for diffraction peaks over the angular range of $2\Theta = 5^{\circ}$ to 80° using Bruker AXS D8 Advance diffractometer with Cu Kα radiation source ($\lambda = 1.54060$ Å) with a scan speed of $5^{\circ}C/min$ and an operating voltage of 40 kV at 30 mA current. The ^{1}H NMR spectra were recorded with an NMR spectrometer (Bruker, 500 MHz) in deuterated DMSO (DMSO-d_6) and recorded chemical shifts are in parts per million (ppm) versus tetramethylsilane (TMS). Thermogravimetric analysis was performed with a NETZSCH TG 209F1 Libra TGA209F1D-0105-L to explore thermal stability of SPEEK under nitrogen atmosphere with a heating rate of 10 °C/min from 70–800 °C. If not stated otherwise, experiments were performed at 20 ± 2 °C.

Synthesis of Semipermeable SPEEK Ionomer

The polymeric backbone of PEEK was altered by the addition of sulfonic acid group ($-SO_3^-$) in the presence of sulfuric acid (18 M) as reported previously.[40,41] Briefly, the reaction mixture PEEK: H_2SO_4 (1:10 w/v) was allowed to react for 18.5 hours under vigorous mechanical stirring at room temperature. Afterwards, the viscous deep reddish-brown solution was precipitated by a phase inversion method by slowly adding it into a bucket full of icy chilled DI water (be careful to avoid heating). This gives SPEEK in noodle-like form, which is easy to filter and wash. The washing must continue until pH reaches neutral. The sulfonic acid group functionalized material is then dried at 70 °C (overnight) to remove excess moisture. Data from FTIR (Figure S1), ^{1}H-NMR (Figure S2), XRD (Figure S3), and thermogravimetry (Figure S4) are provided in the supporting information. The degree of sulfonation is estimated to be 50%.

Ionic Diode Preparation

Membrane preparation was based on SPEEK polymer was dissolved in NMP with a concentration of 1 wt% SPEEK. The Teflon film with microhole was placed on a glass substrate, which was coated with 1 wt. % agarose gel, to prevent the chloroform solution from penetrating through the microhole. A volume of 10 μL of the solution was then deposited onto the microhole area of the Teflon substrate. After evaporation (12 h), this produced a membrane coating with a typical thickness of 0.7 ± 0.3 μm (see cross-sectional SEM below in Figure 3).

2. Results and Discussion

2.1. SPEEK Ionic Diodes in Aqueous NaCl

Cyclic voltammetry experiments (4-electrode mode; see cell in Figure 1B) for the SPEEK film on a Teflon substrate (5 μm thickness, 10 μm diameter microhole) provide clear evidence for an ionic diode effect. Figure 4A shows data for a scan rate of 10 $mV\,s^{-1}$ with a closed diode in the negative potential range

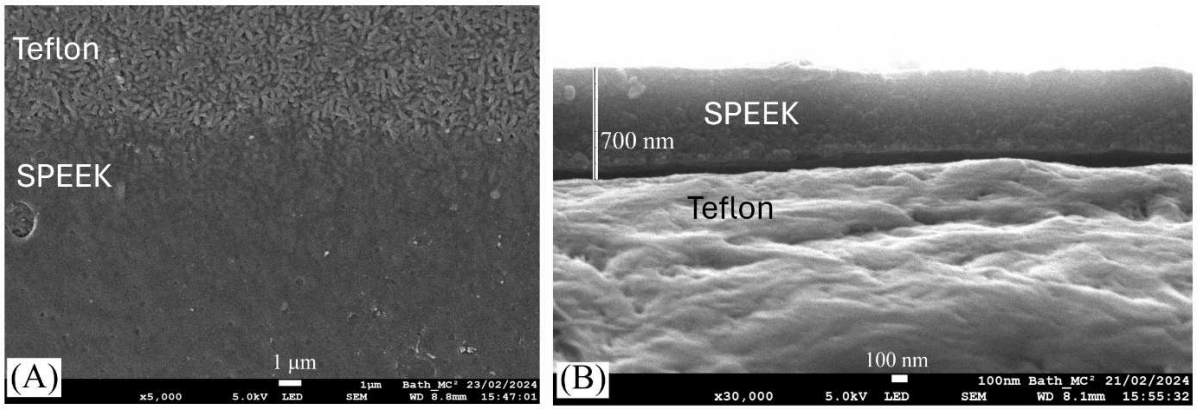

Figure 3. Scanning electron microscopy (SEM) images for (A) the top view of a layer of SPEEK on Teflon (bottom) and bare Teflon revealing some crystalline regions (top). (B) Cross-sectional view of SPEEK on Teflon.

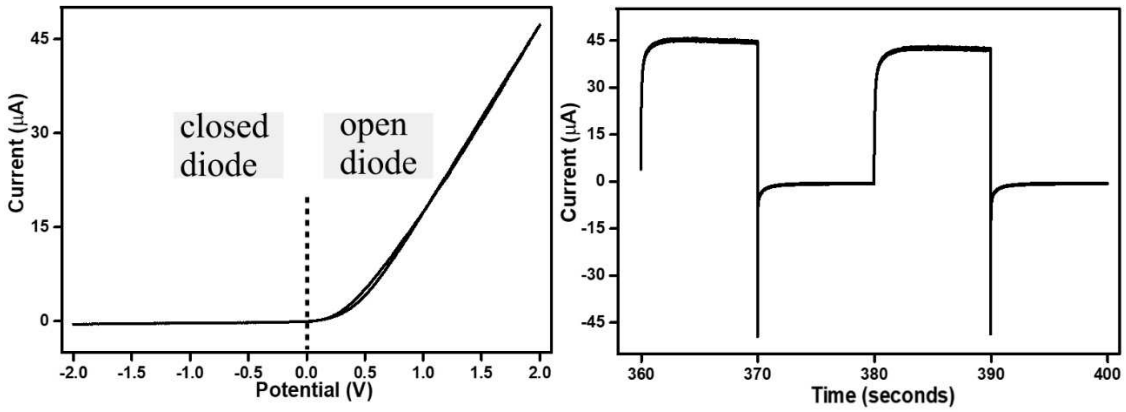

Figure 4. (A) Cyclic voltammograms (4-electrode configuration; scan rate 10 mV s^{-1}) for a SPEEK ionic diode (on Teflon, 5 μm thickness, 10 μm diameter microhole) in aqueous 10 mM NaCl on both sides. (B) Chronoamperometry data obtained at ± 2 V.

and an open diode in the positive potential range. Chronoamperometry data are shown in Figure 4B to confirm this result.

An open diode in the positive potential region implies cation transport. Similar to the case of Nafion,[21] SPEEK is a cation conductor. With positive potential applied to the working electrode, a flow of cations via the membrane into the microhole triggers an increase in local electrolyte concentration (accumulation) in the microhole leading to a high conductivity and high current (open diode) as illustrated in Figure 2A/B (concentration polarisation). However, currents observed for SPEEK are relatively low (compare to graphene oxide cationic diodes[22]) and therefore concentration polarisation seems less likely as a dominant mechanism.

Alternatively, the electrolyte depletion/accumulation in the microhole region could be less important. Cations may flow through the resistive membrane at positive applied potentials (*i.e.* open diode conditions but the currents are limited). Then, with negative applied potentials, depletion of electrolyte occurs within the membrane as a depletion of cationic charge carriers from the membrane (hypothetically important for rigid polymer structures and for lower currents; interfacial polarisation, see Figure 2C).

2.2. SPEEK Ionic Diodes in Aqueous NaCl: Concentration Effects

When investigating the effect of the electrolyte concentration, unusually small changes in the diode current are observed. Figures 5 and 6 show typical data sets based on voltammetry and chronoamperometry. Figure 6A demonstrates that changing the NaCl concentration over more than 2 orders of magnitude only causes a minor change in open diode current. In previous reports typically linear increases in current (for both open and closed diodes) were observed and explained based on theory for concentration polarisation.[22] Here, a two order of magnitude increase in NaCl concentration only leads to doubling of the current (Figure 5A). These ionic diode currents

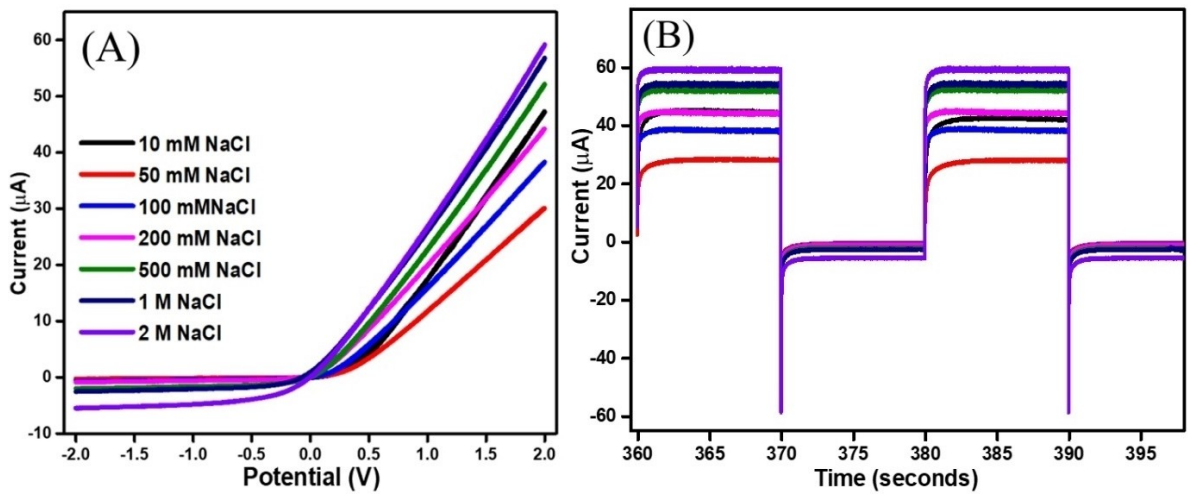

Figure 5. (A) Cyclic voltammograms (4-electrode configuration; scan rate 10 mV s^{-1}) for a SPEEK ionic diode (on Teflon, 5 μm thickness, 10 μm diameter microhole) in aqueous (i) 10 (ii) 50 (iii) 100 (iv) 200 (v) 500 (vi) 1000, and (vii) 2000 mM NaCl on both sides. (B) Chronoamperometry data obtained by stepping the voltage between ± 2 V.

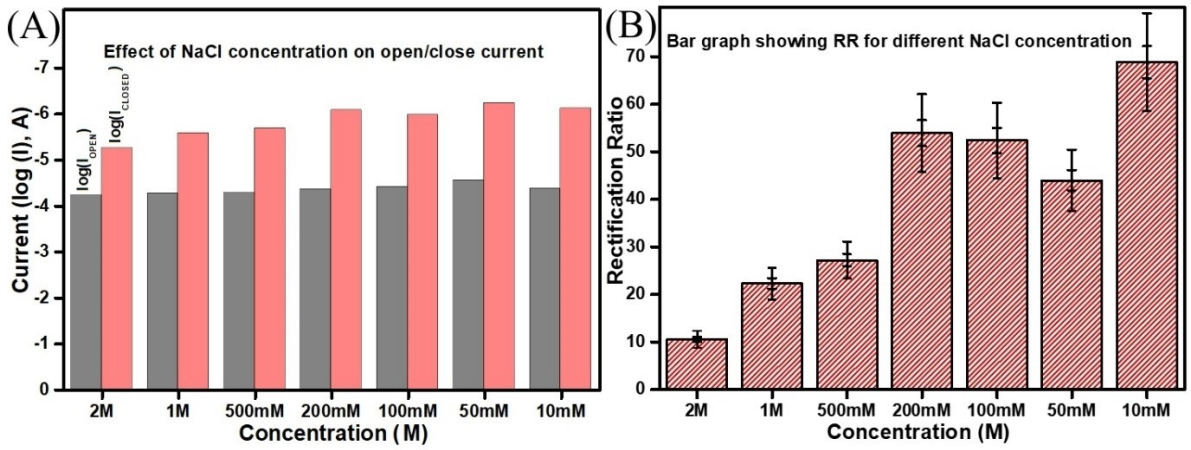

Figure 6. (A) Bar graph showing the logarithm of diode currents (from chronoamperometry at ±2 V) as a function of NaCl concentration. (B) Bar graph showing the rectification ratio as a function of NaCl concentration (errors ±3σ for 3 repeats).

at high ionic strengths are generally lower compared to those observed for similar types of diodes and conditions. This suggests that concentration polarisation is less likely as a diode mechanism. However, the rectification ratio data remain promising even up to 2 M NaCl (Figure 6B).

Chronoamperometry data in Figure 5B suggest fast switching from open to closed and back to open diode state (within <1 s). Both switching time and transient shape appear to be independent of the electrolyte concentration. The transient time has been related to the limiting diffusion-migration time for electrolyte into/out of the microhole region.[21]

High electrolyte concentration performance of ionic diodes is important. Applications linked to brine or to sea water require high rectification ratios even at high ionic strengths. The rectification ratio data for SPEEK are very promising and outstanding at high ionic strengths when compared to other types of ionic diode systems. These SPEEK ionic diodes are unlikely to operate with a mechanism based purely on concentration polarisation. Therefore, a new/additional type of mechanism based on interfacial polarisation is proposed for SPEEK.

2.3. SPEEK Ionic Diodes in Aqueous Electrolytes: HCl, LiCl, NaCl, $MgCl_2$

In preliminary work, different types of aqueous electrolytes were investigated. Figure 7 shows data contrasting diode behaviour in aqueous 10 mM NaCl, HCl, LiCl, and $MgCl_2$. In all cases cationic diodes are observed (for cation conducting SPEEK). Due to a high mobility of protons, the currents for 10 mM HCl are enhanced when compared to aqueous NaCl. LiCl and NaCl appear to be very similar in ionic diode behaviour. A slight increase in open diode current for $MgCl_2$ could be linked to a higher ionic strength or (perhaps more likely) enhanced charge mobility within the SPEEK film. Note, that the change in cation causes significantly higher changes in diode current compared to changes due to electrolyte concentration (Figure 7).

It is interesting to explore the ionic diode behaviour at higher applied voltages. Data in Figure 7C reveal cationic diode behaviour up to ±7 V without any signs of detrimental (or break-down) effects. The rectification ratio increases significantly at higher voltages. A non-linear increase in current at

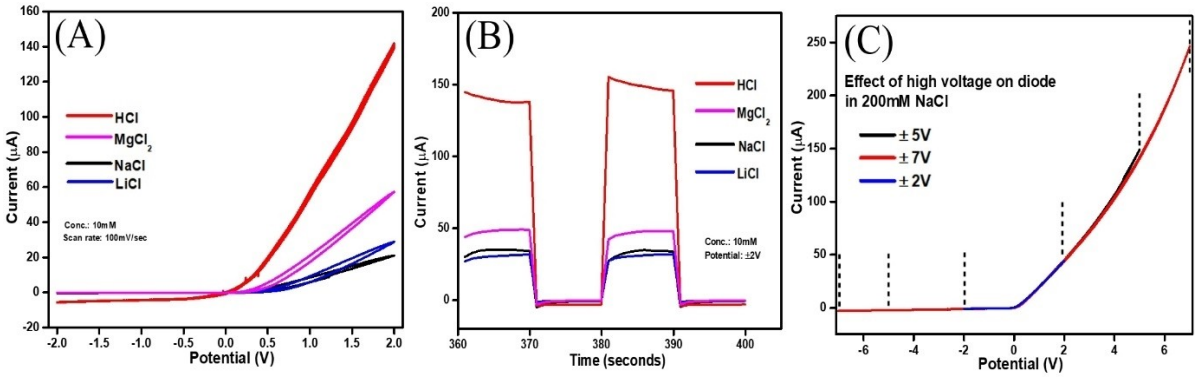

Figure 7. (A) Cyclic voltammograms (4-electrode configuration; scan rate 10 mV s^{-1}) for a SPEEK ionic diode (on Teflon, 5 μm thickness, with 10 μm diameter microhole) in aqueous 10 mM (i) HCl, (ii) $MgCl_2$, (iii) NaCl, and (iv) LiCl on both sides. (B) Chronoamperometry data obtained at ±2 V. (C) Cyclic voltammetry data (4-electrode configuration; scan rate 10 mV s^{-1}) demonstrating ionic diode performance for 200 mM NaCl at higher voltages.

+4 V can be attributed to the onset of electroconvection (overlimiting conditions[42,43,44]).

The SPEEK ionic diode behaviour is interesting due to the observation that both processes, (I) within the electrolyte solution (concentration polarisation) and (II) processes within the polymer membrane (interfacial polarisation), are in part responsible for the diode phenomenon. This decreases the effect of ionic strength on rectification, and it allows rectification to be observed even at high salt concentrations (even at 2 M NaCl). More importantly, phenomena within the polymer increase cation (the mobile species) selectivity effects. The transport of cations in the SPEEK cationic diode follows a decreasing trend for $H^+ > Mg^{2+} > Li^+ > Na^+$, which could be associated with cation selectivity/mobility within the ionomer. In the future, cation selectivity could be employed to make ionic diodes selective to remove specific types of cations (e.g. Li^+) in the presence of excess solution electrolyte. This is not possible with the concentration polarisation mechanism (ionic strength dependent without selectivity), but it will be possible with the interfacial polarisation mechanism (ionic strength independent with selectivity for specific cations).

The ionic diode mechanism is important in terms of current and rectification. Figure 8 illustrates the proposed transition from concentration polarisation to interfacial polarisation depending on the interaction of ion and ionomer. Further understanding of the impact of ionomer material type and molecular structure/rigidity on rectification and on ion selectivity will be important for future exploitation of time dependent phenomena and of ion selectivity effects in ionic diode devices and in ionic circuits.

3. Conclusions

The ionomer SPEEK has been investigated as thin film semi-permeable ionic diode material in microhole devices. The sulfonate group in the polymer causes cationic conductivity and changes in diode current depending on the type of cation. A film of typically 700 nm SPEEK asymmetrically deposited onto a Teflon substrate with 10 μm diameter microhole, shows cationic diode properties, which persist even at increased levels of ionic strength (up to 2 M NaCl). A preliminary investigation of different types of cations suggests that cation - ionomer interactions are important. However, for a better understanding more data for a wider range of cations and conditions will be necessary. Additional work on device design and stability under operational conditions will be important in the future.

The mechanism for the SPEEK ionic diode will require further study and better computational approaches (beyond finite element methods) will be required to elucidate the effects of polymer molecular structure (at atomistic level) on ionic diode performance. The pore structure of the ionomer and the charge distribution are linked to interfacial polarisation phenomena. Atomistic computational models could help predicting good ionic diode materials and predicting ion selectivity for diodes that target specific ions.

Potential implications of the current work for practical applications of ionic diode processes are mainly linked to the interfacial polarisation mechanism being based on interaction of cations with the ionomer material (and not simply concentration polarisation). This allows new ionomer materials to be developed and synthesised in the future with even higher rectification effect or with improved ion selectivity (e.g. selecting for lithium cations for lithium enrichment).

The observation of interfacial polarisation effects and direct effects of ionomer material on cation transport and rectification ratio are promising for applications that require performance in high ionic strength environments and/or for high selectivity towards specific types of ions. This study of SPEEK as an ionic diode material suggests that there are further opportunities based on developing new and optimised (molecularly rigid) microporous ionomer materials.

Acknowledgements

F.M. thanks for the initial financial support by the EPSRC (EP/K004956/1). C.S. is thankful to the Commonwealth Scholarship Commission (CSC, split-site fellowship, grant: INCN-22-437) and the Ministry of Human Resources (MHRD), India, for financial

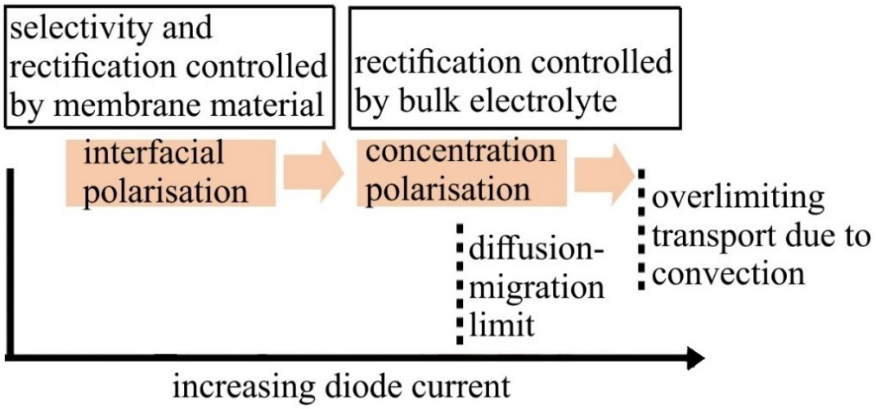

Figure 8. Schematic description of the transition from interfacial polarisation (low ionic diode current) to concentration polarisation (high ionic diode current) with a further increase in current possible due to overlimiting conditions.

assistance. We thank the University of Bath for support to perform this research work.

Conflict of Interests

The authors declare no conflict of interest.

Data Availability Statement

The data that support the findings of this study are available from the corresponding author upon reasonable request.

Keywords: Nanofluidic diode · Desalination · Ionic circuits · Ionic logic · Voltammetry

[1] H. J. Koo, O. D. Velev, *Biomicrofluidics* **2013**, *7*(3), 031501, DOI: 10.1063/1.4804249.
[2] X. Hou, W. Guo, L. Jiang, *Chem. Soc. Rev.* **2011**, *40*(5), 2385–2401, DOI: 10.1039/c0cs00053a.
[3] B. R. Putra, L. Tshwenya, M. A. Buckingham, J. Y. Chen, K. J. Aoki, K. Mathwig, O. A. Arotiba, A. K. Thompson, Z. K. Li, F. Marken, *Electroanalysis* **2021**, *33*(6), 1398–1418, DOI: 10.1002/elan.202060614.
[4] W. Guo, Y. Tian, L. Jiang, *Acc. Chem. Res.* **2013**, *46*(12), 2834–2846, DOI: 10.1021/ar400024p.
[5] C. Kubeil, A. Bund, *J. Phys. Chem. C* **2011**, *115*(16), 7866–7873, DOI: 10.1021/jp111377h.
[6] T. J. Liu, T. J. Ma, C. Y. Lin, S. Balme, J. P. Hsu, *J. Phys. Chem. Lett.* **2021**, *12*(49), 11858–11864, DOI: 10.1021/acs.jpclett.1c03513.
[7] S. D. Zhang, X. H. Yin, M. Z. Li, X. H. Zhang, X. Zhang, X. L. Qin, Z. W. Zhu, S. Yang, Y. H. Shao, *Anal. Chem.* **2018**, *90*(14), 8592–8599, DOI: 10.1021/acs.analchem.8b01765.
[8] L. Yang, J. Hu, M. C. Li, M. Xu, Z. Y. Gu, *Chem. Asian J.* **2022**, *17*(22), e202200775, DOI: 10.1002/asia.202200775.
[9] Z. Zhang, L. P. Wen, L. Jiang, *Chem. Soc. Rev.* **2018**, *47*(2), 322–356, DOI: 10.1039/c7cs00688h.
[10] H. G. Chun, T. D. Chung, *Ann. Rev. Anal. Chem.* **2015**, *8*, 441–462, DOI: 10.1146/annurev-anchem-071114-040202.
[11] K. J. Aoki, L. Liu, F. Marken, J. Y. Chen, *Electrochim. Acta* **2020**, *358*, 136839, DOI: 10.1016/j.electacta.2020.136839.
[12] B. Lovrecek, A. Despic, J. O. M. Bockris, *J. Phys. Chem.* **1959**, *63*(5), 750–751, DOI: 10.1021/j150575a030.
[13] B. R. Putra, M. Carta, R. Malpass-Evans, N. B. McKeown, F. Marken, *Electrochim. Acta* **2017**, *258*, 807–813, DOI: 10.1016/j.electacta.2017.11.130.
[14] B. R. Putra, E. Madrid, L. Tshwenya, O. A. Arotiba, F. Marken, *Desalination* **2020**, *480*, 114351, DOI: 10.1016/j.desal.2020.114351.
[15] D. L. Ramada, J. de Vries, J. Vollenbroek, N. Noor, O. ter Beek, S. M. Mihăilă, F. Wieringa, R. Masereeuw, K. Gerritsen, D. Stamatialis *Nature Rev. Nephrology* **2023**, *19*, 481–490, DOI: 10.1038/s41581-023-00726-9.
[16] Z. K. Li, J. P. Lowe, P. J. Fletcher, M. Carta, N. B. McKeown, F. Marken, *ACS Appl. Mater. Interfaces* **2023**, *15*(36), 42369–42377, DOI: 10.1021/acsami.3c10220.
[17] D. Zhang, X. J. Zhang, *Small* **2021**, *17*(43), 2100495, DOI: 10.1002/smll.202100495.
[18] D. Duleba, R. P. Johnson, *Curr. Opinion Electrochem.* **2022**, *34*, 100989, DOI: 10.1016/j.coelec.2022.100989.
[19] B. Sabbagh, N. E. Fraiman, A. Fish, G. Yossifon, *ACS Appl. Mater. Interfaces* **2023**, *15*(19), 23361–23370, DOI: 10.1021/acsami.3c00062.
[20] Z. K. Li, K. Mathwig, O. A. Arotiba, L. Tshwenya, E. B. C. Neto, E. C. Pereira, F. Marken, *Curr. Opinion Electrochem.* **2023**, *39*, 101280, DOI: 10.1016/j.coelec.2023.101280.
[21] S. Park, G. Yossifon, *Nanoscale* **2018**, *10*(24), 11633–11641, DOI: 10.1039/c8nr02389a.
[22] M. A. Alkhadra, X. Su, M. E. Suss, H. H. Tian, E. N. Guyes, A. N. Shocron, K. M. Conforti, J. P. De Souza, N. Kim, M. Tedesco, K. Khoiruddin, I. G. Wenten, J. G. Santiago, T. A. Hatton, M. Z. Bazant, *Chem. Rev.* **2022**, DOI: 10.1021/acs.chemrev.1c00396.
[23] J. Gao, W. Guo, D. Feng, H. T. Wang, D. Y. Zhao, L. Jiang, *J. Amer. Chem. Soc.* **2014**, *136*(35), 12265–12272, DOI: 10.1021/ja503692z.
[24] B. Sabbagh, N. E. Fraiman, A. Fish, G. Yossifon, *ACS Appl. Mater. Interfaces* **2023**, *15*(19), 23361–23370, DOI: 10.1021/acsami.3c00062.
[25] E. Madrid, Y. Y. Rong, M. Carta, N. B. McKeown, R. Malpass-Evans, G. A. Attard, T. J. Clarke, S. H. Taylor, Y. T. Long, F. Marken, *Angew. Chem. Inter. Ed.* **2014**, *53*(40), 10751–10754, DOI: 10.1002/anie.201405755.
[26] D. P. He, E. Madrid, B. D. B. Aaronson, L. Fan, J. Doughty, K. Mathwig, A. M. Bond, N. B. McKeown, F. Marken, *ACS Appl. Mater. Interfaces* **2017**, *9*(12), 11272–11278, DOI: 10.1021/acsami.7b01774.
[27] B. R. Putra, K. J. Aoki, J. Y. Chen, F. Marken, *Langmuir* **2019**, *35*(6), 2055–2065, DOI: 10.1021/acs.langmuir.8b03223.
[28] E. B. Carneiro-Neto, Z. K. Li, E. Pereira, K. Mathwig, P. J. Fletcher, F. Marken, *ACS Appl. Mater. Interfaces* **2023**, *15*(33), 39905–39914, DOI: 10.1021/acsami.3c08543.
[29] Z. K. Li, T. T. Pang, J. J. Shen, P. J. Fletcher, K. Mathwig, F. Marken, *Micro Nano Eng.* **2022**, *16*, 100157, DOI: 10.1016/j.mne.2022.100157.
[30] B. R. Putra, K. Szot-Karpinska, P. Kudla, H. Yin, J. A. Boswell, A. J. Squires, M. A. Da Silva, K. J. Edler, P. J. Fletcher, S. C. Parker, F. Marken, *ACS Appl. Bio Mater.* **2020**, *3*(1), 512–521, DOI: 10.1021/acsabm.9b00952.
[31] Z. K. Li, M. Carta, N. B. McKeown, R. E. Agbenyeke, J. C. Eloi, D. J. Fermin, O. A. Arotiba, F. Marken, *ChemElectroChem* **2024**, DOI: 10.1002/celc.202300807.
[32] B. M. Mahimai, G. M. Sivasubramanian, K. Sekar, D. Kannaiyan, P. Deivanayagam, *Mater. Adv.* **2022**, *3*, 6085–6095, DOI: 10.1039/d2ma00562j.
[33] C. K. Jia, J. G. Liu, C. W. Yan, *J. Power Sources* **2010**, *195*(13), 4380–4383, DOI: 10.1016/j.jpowsour.2010.02.008.
[34] H. Sijbesma, K. Nymeijer, R. van Marwijk, R. Heijboer, J. Potreck, M. Wessling, *J. Membrane Sci.* **2008**, *313*(1–2), 263–276, DOI: 10.1016/j.memsci.2008.01.024.
[35] P. H. Qian, H. X. Wang, L. Zhang, Y. Zhou, H. F. Shi, *J. Membrane Sci.* **2022**, *643*, 120011, DOI: 10.1016/j.memsci.2024.122663.
[36] X. Jin, M. T. Bishop, T. S. Ellis, *British Polymer J.* **1985**, *17*, 4–10, DOI: 10.1002/pi.4980170102.
[37] J. Leddy, *Nanomater. Sust. Energy* **2015**, *1213*, 99–133, DOI: 10.1021/bk-2015-1213.ch006.
[38] K. Mathwig, B. D. B. Aaronson, F. Marken, *ChemElectroChem* **2018**, *5*(6), 897–901, DOI: 10.1002/celc.201700464.
[39] E. B. Carneiro-Neto, Z. K. Li, E. Pereira, K. Mathwig, P. J. Fletcher, F. Marken, *ACS Appl. Mater. Interfaces* **2023**, DOI: 10.1021/acsami.3c08543.
[40] T. K. Maiti, J. Singh, S. K. Maiti, A. Ahuja, P. Dixit, J. Majhi, A. Bandyopadhyay, S. Chattopadhyay, *J. Solid State Electrochem.* **2022**, *26*, 2565–2583, DOI: 10.1007/s10008-022-05276-x.
[41] B. Eswaraswamy, P. Mandal, P. Goel, S. Chattopadhyay, *ACS Appl. Polym. Mater.* **2021**, *3*(12), 6218–6229, DOI: 10.1021/acsapm.1c01045.
[42] I. Rubinstein, L. Shtilman, *J. Chem. Soc. Faraday Trans.* II **1979**, *75*, 231–246, DOI: 10.1039/f29797500231.
[43] E. V. Dydek, B. Zaltzman, I. Rubinstein, D. S. Deng, A. Mani, M. Z. Bazant, *Phys. Rev. Lett.* **2011**, *107*(11), 118301, DOI: 10.1103/PhysRevLett.107.118301.
[44] V. V. Nikonenko, A. V. Kovalenko, M. K. Urtenov, N. D. Pismenskaya, J. Han, P. Sistat, G. Pourcelly, *Desalination* **2014**, *342*, 85–106, DOI: 10.1016/j.desal.2014.01.008.

Manuscript received: June 11, 2024
Revised manuscript received: July 3, 2024
Version of record online: September 5, 2024